Available online at www.sciencedirect.com
SCIENCE DIRECT®

Nuclear Science and Techniques, Vol.17, No.1 (2006) 1–6

NUCLEAR SCIENCE AND TECHNIQUES

# Effects of insertion device on SSRF storage ring

ZHANG Li-Hua LIAO Yi LIU Gui-Min

*(Shanghai Institute of Applied Physics, the Chinese Academy of Sciences, Shanghai 201800, China)*

**Abstract** Shanghai Synchrotron Radiation Facility (SSRF), one of the third generation light sources, aims to produce high brightness and/or high flux X-ray source for users; therefore insertion devices (IDs) are important magnetic elements for SSRF. In this paper, the linear perturbations due to IDs toward its storage ring lattice, such as beta function distortions, tune shifts, emittance growths, and energy spreads are estimated by using analytical formulae, and the nonlinear effects from IDs, especially dynamic aperture, are simulated by using Racetrack code. The results show that (a) the reduction of dynamic aperture from single undulator is negligible, since electron beam energy of 3.5 GeV is high and ID's magnetic field is low, and the beta functions in the middle of straight sections, where ID is located, are well optimized; (b) however, the reduction from single wigglers, especially super-conducting wiggler, is visible, because of its higher magnetic field; (c) effects of each ID on emittance growths and energy spreads are less than 7%.

**Key words** SSRF, Insertion devices, Linear optics distortion, Compensation, Dynamic aperture

**CLC number** TL593

## 1 Introduction

Shanghai Synchrotron Radiation Facility (SSRF) is a third generation synchrotron light source with beam energy of 3.5 GeV in Shanghai, China. The storage ring has 16 standard sections of 6.5 meters long and 4 long sections of 12 meters long, and its circumference is 432 meters. Like most of the third generation synchrotron radiation light sources [1-4], SSRF will finally adopt more than eighteen insertion devices (wigglers and undulators). Due to the limited budget, it has been planned that only four IDs will be constructed at the first stage of SSRF, i.e. one multipole wiggler (MPW), two min-gap undulators (U27), and one normal undulator (U90) while one or two superconducting wiggler (SW) will be considered in the future, as listed in Table 1.These four kinds of IDs cover all the typical demonstrations of the IDs except the elliptical polarized undulators (EPU).

Insertion device is a periodical magnetic element[5]. Its magnetic field will provide an additional focusing force on the electron beam in one or two directions, resulting in beta-function distortions, tune shifts, and broken symmetry. Meanwhile, ID itself is a nonlinear element and further increases the nonlinearity of the ring lattice, resulting in an additional nonlinear resonance and making dynamic aperture smaller. Moreover, the radiation damping and quantum excitation processes for electron beam can be affected by the dipole component of IDs, causing an increase in beam emittance and energy spread. Therefore, the effects of IDs could be harmful to the performance of the machine and should be calculated and even compensated. In this paper, the dynamic aperture of the ring lattice with IDs is simulated, and the beta function distortions, tune shifts, emittance growths, and energy spreads due to IDs are calculated.

## 2 Optics distortion and dynamic aperture reduction

### 2.1 Optics distortion and compensation

The effects from each single ID on linear optics

Received date: 2004-10-15

are calculated by the analytical formula and compared with the results from Racetrack code simulation, shown in Table 1. Insertion devices, U27, MPW, U90 and SW, are installed in the standard sections, and the insertion device, double U90, is installed in the long section. Table 1 shows that the SW's effect on linear optics distortions is larger than the others, because of its highest magnetic field.

**Table 1** Parameters of IDs and linear optics distortions

| ID | $B_0$ / T | $L_u$ / m | $N_u$ | $\lambda_u$ / m | $g$ / mm | $\beta_y$ / m | $\Delta\nu_y$ | $\Delta\beta_y/\beta_y$ (%) |
|---|---|---|---|---|---|---|---|---|
| U27 | 0.8 | 2.0 | 74 | 0.027 | 7.0 | 2.5 | 0.0010 | — |
| MPW | 1.47 | 2.0 | 20 | 0.1 | | 2.5 | 0.0032 | — |
| U90 | 0.344 | 4.5 | 50 | 0.09 | 48.9 | 2.5 | 0.00038 | — |
| SW | 4.2 | 0.74 | 4 | 0.185 | | 2.5 | 0.0099 | 2.4 |
| 2×U90 | 0.344 | 9.0 | 100 | 0.09 | 48.9 | 2.5 | 0.00076 | — |

The results from Racetrack code simulation agree quite well with that from theoretical analysis. The additional focusing component[6] from an insertion device is determined by

$$K_{Q_{x,y}} = \frac{1}{2}\left(\frac{k_{x,y}}{\rho k}\right)^2 \qquad (1)$$

where $k_x^2 + k_y^2 = k^2 = \left(\frac{2\pi}{\lambda}\right)^2$, $\rho$ is the bending radius of ID's peak field $B_0$. For normal plane polarized ID, $k_x$=0, so only vertical focusing force exists. From the above formula, it can be seen that the focusing force is proportional to $B^2/E^2$, so the SW's effect is larger than the others because of its higher magnetic field. The vertical tune shift of the optics is

$$\Delta\upsilon_y \approx \frac{\beta_y L_{\mathrm{ID}}}{8\pi\rho^2} \qquad (2)$$

According to Eq. (2), ID's effects on tune shifts are calculated, which are almost the same as the results from the simulation results by Racetrack code.

The linear optics distortions are compensated locally via adjusting the focusing strengths of two quadrupole pairs, Q1 and Q2, located beside each ID. The changes in each of the two quadrupole pairs' strengths are summarized in Table 2.

**Table 2** Changes in quadrupole pair's strengths for local compensations

| Quad. | | U27 | MPW | U90 | SW* | 2×U90 |
|---|---|---|---|---|---|---|
| Q1 | Original / $m^{-2}$ | 1.48996 | 1.48996 | 1.48996 | 1.48996 | 1.05188 |
| | Matched / $m^{-2}$ | 1.49502 | 1.50271 | 1.49172 | 1.51470 | 1.02895 |
| | Change / % | 0.34 | 0.86 | 0.12 | 1.66 | 2.18 |
| Q2/Q3 | Original / $m^{-2}$ | −1.46384 | −1.46384 | −1.46384 | 0.68195* | −1.26218 |
| | Matched / $m^{-2}$ | −1.46293 | −1.45941 | −1.46363 | 0.70483 | −1.25308 |
| | Change / % | −0.06 | −0.30 | −0.01 | 3.36 | 0.72 |

* For SW, the quadrupole-pairs are Q1 and Q3 shown as follows:

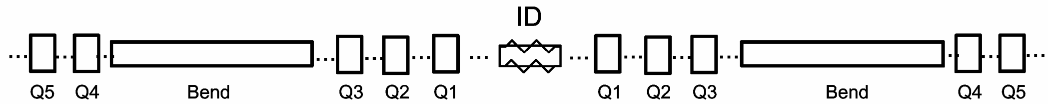


The beta function distortions for each single ID have been simulated before/after compensations. Because SW has the highest magnetic field and the largest beta function distortions, its result is shown in Fig.1. It can be seen that horizontal beta function $\beta_x$ with SW before/after compensations is the same because SW is a vertical plane polarized insertion device, and can only afford vertical focusing force.

Without compensations, the tune shifts are 0.001, 0.003, 0.0004, 0.0008, and 0.01 for U27, MPW, U90, $2\times$U90, and SW, respectively. After local compensation, i.e. alpha matching, the tune shifts are 0.003, 0.01, 0.001, -0.005, and 0.024, respectively. The changes are small even for SW. As a result, the working point in the resonance diagram does not change too much, so the tune need not be adjusted.

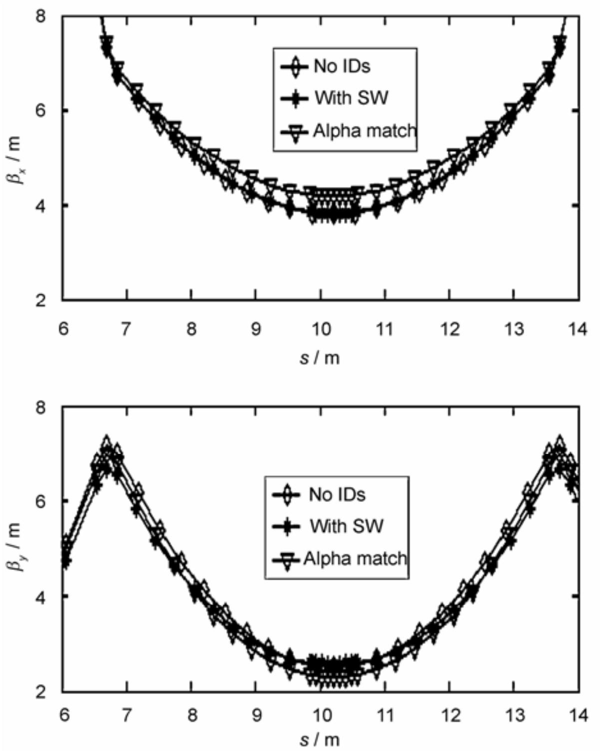


**Fig.1** SW's effect on beta-function.

## 2.2 Dynamic aperture reduction

The effects of IDs on dynamic aperture can be investigated by tracking particles through the ring lattice element by element, and the parameters of the insertion device are described as above. In Racetrack code, the insertion device is sliced into several segments per period with the nonlinear terms averaged over each slice and applied as thin kicks. The code has two different integration schemes. One is second-order symplectic insertion device transformation based on Taylor's series expansion, the other is conventional second-order symplectic insertion device integration.[7] Therefore, we use Racetrack code to simulate each ID's effect on dynamic aperture in detail. The results are shown in Fig.2 to Fig.5. Fig.6 shows how the double U90 undulator, assumed to be installed in the long section of 12m, affects dynamic aperture. Fig.7 shows all SSRF IDs' effects on dynamic aperture. All the results show that SSRF IDs, at least in the first stage, do not affect dynamic aperture much. Dynamical aperture with all the IDs together is larger than the physical aperture, so effects of IDs are negligible. As far as the case with all the IDs is concerned, the dynamic aperture will be reduced further.

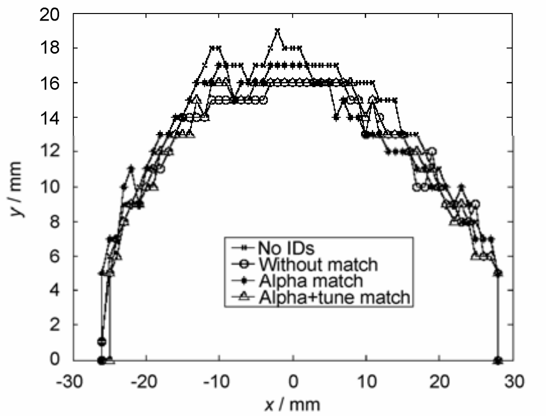


**Fig.2** ID-U27's effect on dynamic aperture.

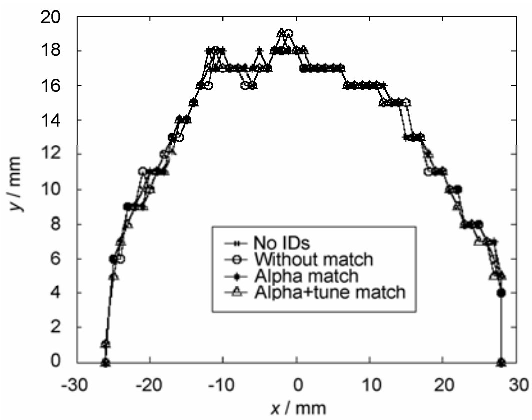


**Fig.3** ID-U90's effect on dynamic aperture.

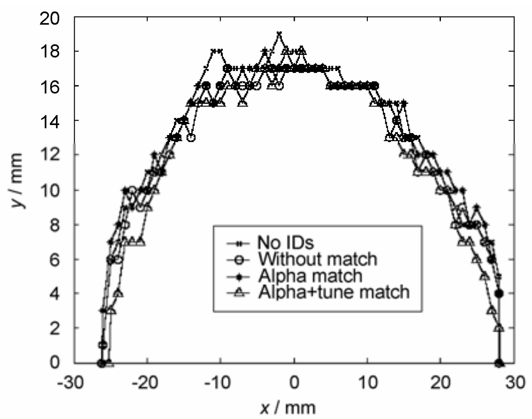


**Fig.4** MPW's effect on dynamic aperture.

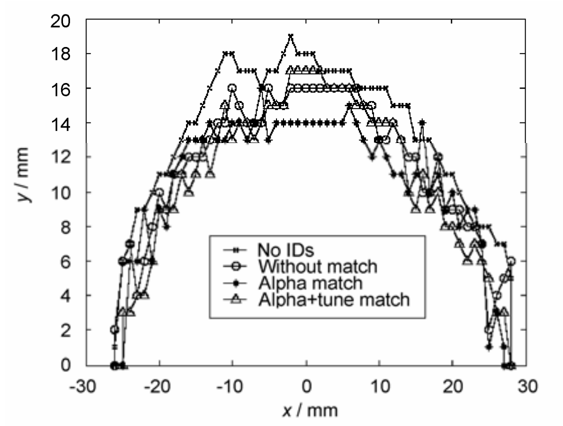


**Fig.5** SW's effect on dynamic aperture.

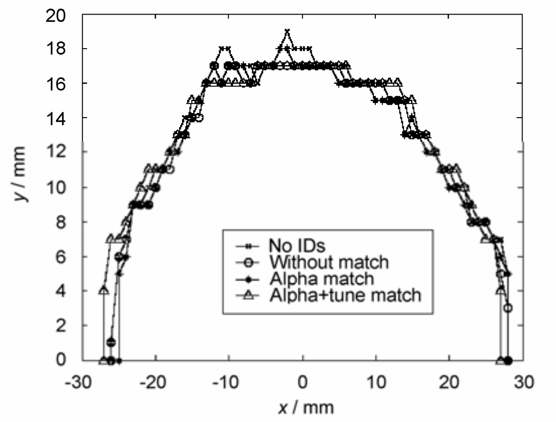


**Fig.6** 2×U90's effect on dynamic aperture (installed in super long section).

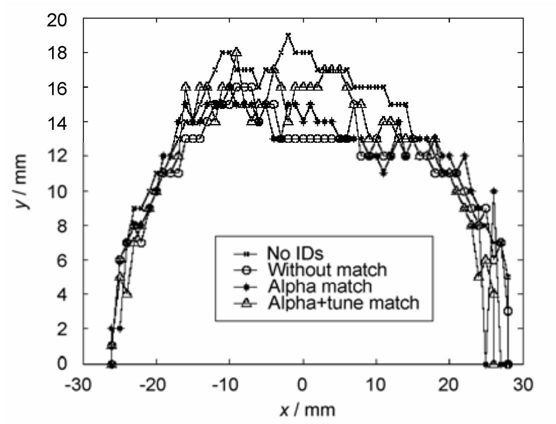


**Fig.7** SSRF first stage IDs' effect on dynamic aperture (two U27, one U90, one MPW).

It turns out that higher energy machines are less affected than lower energy ones, which is mainly due to the fact that the nonlinear terms scale as $\rho^{-2}$. One can see that the increase in nonlinearity is inversely proportional to $\sqrt{\lambda}$ [8]. Stronger nonlinearity will introduce additional resonance, then chromaticity correction must be made again by optimizing sextupoles' strengths.

## 3 Growth of emittance and energy spread

### 3.1 Energy loss

Relativistic electrons will loss energy when passing through IDs or dipoles. An electron's radiation power when moving along a curve is given by[9]

$$P_r = \frac{2e^2 c}{3\rho^2}\beta_v^4 \gamma^4 \tag{3}$$

where $\rho$ is the radius of curve in the field $B_0$, $\beta_v$ is relativistic velocity, $\gamma$ is relativistic energy. For high energy electron beam, the relativistic velocity is almost equal to 1. We can define a constant

$$C_r = \frac{4\pi}{3} \times \frac{r_e}{(m_0 c^2)^3} = 8.85 \times 10^{-5} (\mathrm{m \cdot GeV^{-3}}) \tag{4}$$

where $r_e = \dfrac{e^2}{m_0 c^2}$ is the classical electron radius, $m_0 c^2$ is the electron rest energy. After inserting this constant into the above formula, we can get the well-known form for radiation power:

$$P_r = \frac{c C_r E^4}{2\pi} / \rho^2(s) \tag{5}$$

where $E$ is the nominal energy of the stored electrons. Using the above formula, the energy loss per turn in an isomagnetic guide field is:

$$U_0 = \int_0^{T_0} P_r \mathrm{d}t = \frac{1}{c}\int P_r \mathrm{d}s = \frac{C_r E^4}{2\pi}\int G^2(s)\mathrm{d}s = \frac{C_r E^4}{\rho_0} \tag{6}$$

Similarly we can get energy loss when electron goes through an ID:

$$U = \frac{L_{\mathrm{ID}}}{4\pi\rho_0}\left(\frac{\rho_0}{\rho}\right)^2 U_0 \tag{7}$$

where $\rho_0$ is electron radius in dipole, $\rho$ is the radius of electron in ID's peak field $B$, $L_{\mathrm{ID}}$ is the length of ID.

Bending magnet and single ID's energy loss per turn are shown in Table 3. There are four IDs as described above at SSRF first stage, i.e. two U27, one MPW, and one U90, thus the total energy loss per turn is 1.5054MeV.

**Table 3** Energy loss, emittance, and energy spread with each ID

| B magnet / ID | Energy loss (MeV/turn) | $\varepsilon_x / \varepsilon_{x0}$ | $\sigma_x / \sigma_{x0}$ |
|---|---|---|---|
| Bending magnet | 1.4480 | — | — |
| U27 | 0.0099 | 0.9929 | 0.9984 |
| MPW | 0.0335 | 0.9765 | 1.0003 |
| U90 | 0.0041 | 0.9970 | 0.9989 |
| SW | 0.1011 | 0.9398 | 1.0632 |

### 3.2 Growth of emittance and energy spread

Due to radiation emission, IDs will generate additional beam emittance and beam energy spread. They can be estimated by the following formulas, and the calculated results are shown in Table 3.

Many of the important properties of the stored beam in an electron storage ring are determined by the so-called synchrotron radiation integrals, taken around the whole ring, of various characteristic functions of the guide field[10]. Beam emittance and beam energy spread are two of the various performance parameters of storage rings that can be expressed in terms of these integrals. The beam emittance and beam energy spread in the bare machine can be expressed by:[1,10]

$$\varepsilon_x = C_q \gamma^2 \frac{I_5}{I_2 - I_4} \tag{8}$$

$$\sigma_\varepsilon = \left( C_q \gamma^2 \frac{I_3}{2I_2 + I_4} \right)^{1/2} \tag{9}$$

where $I_2 = \int \frac{1}{\rho^2} \mathrm{d}s \qquad I_3 = \int \frac{1}{|\rho^3|} \mathrm{d}s$

$$I_4 = \int \frac{1-2n}{\rho^3} \eta \mathrm{d}s \qquad I_5 = \int \frac{H}{|\rho^3|} \mathrm{d}s$$

The introduction of insertion devices will contribute extra terms to these integrals and hence change the beam emittance and beam energy spread, according to:

$$\frac{\varepsilon_x}{\varepsilon_{x0}} = \frac{1 + \sum I_5^{\mathrm{ID}} / I_5^0}{1 + \sum I_2^{\mathrm{ID}} / \sum I_2^0} \tag{10}$$

$$\left( \frac{\sigma_x}{\sigma_{x0}} \right)^2 = \frac{1 + \sum I_3^{\mathrm{ID}} / I_3^0}{1 + \sum I_2^{\mathrm{ID}} / \sum I_2^0} \tag{11}$$

where $I_5^{\mathrm{ID}} \approx \frac{\lambda^2}{15\pi^3 \rho^5} < \beta > L_{\mathrm{ID}}$, which can be gained from programs. Other integrals can be got by analytical computation. Some appropriate approximations have been made in the above formulae. At the first phase of SSRF, the four IDs, i.e. U27, MPW, U90, and SW, are considered to adopt**,** we can get their total effects on emittance and energy spread separately by the above formulas. Their total effects are:

$$\frac{\varepsilon_x}{\varepsilon_{x0}} = 0.9669$$

$$\frac{\sigma_x}{\sigma_{x0}} = 0.9976$$

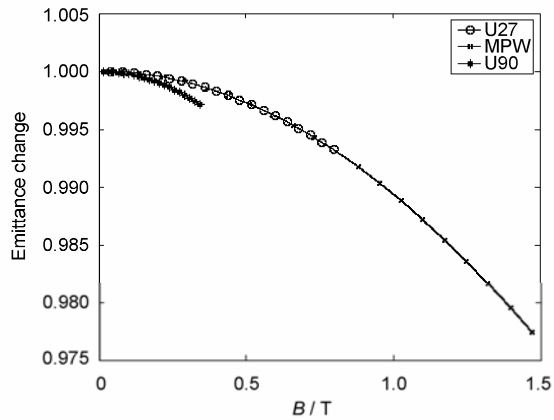


**Fig.8** Single ID's effect on emittance for different field.

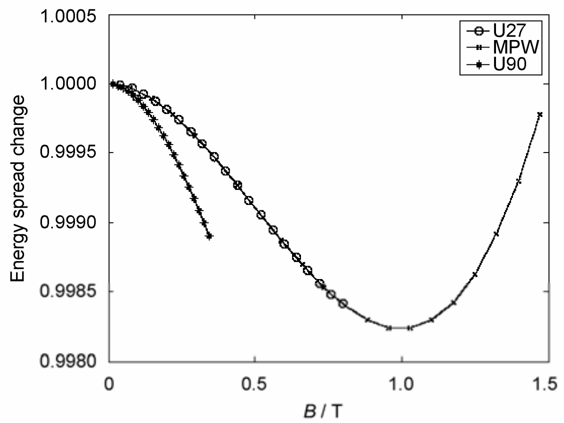


**Fig.9** Single ID's effect on energy spread for different field.

The emittance and energy spread via the field of the insertion device are calculated as shown in Fig.8 and Fig.9. Since the dispersion generated by undulators is usually very small, quantum excitation will be much smaller than the damping effect and the cancellation of energy damping by the increase in quantum fluctuations could occur at high fields. Therefore, for almost all cases of interest, there is a reduction of emittance due to the inclusion of undulators. On the other hand, in low energy machines containing high field wigglers, the self-generated dispersion is dominant and leads to an increase in emittance. The effect on the energy spread is similar to the effect on the emittance. The change in the energy spread depends on the ratio of the magnetic field in the insertion device to that in the bending magnets. Except for low field, there is an increase in the beam energy spread. The following figures also show this conclusion. That is because they have the same length.

The above figures also show that U27's effect and MPW's effect are almost the same, which is attributed to their similar total length and field characteristics. We also studied tune shift behavior as a function of the insertion device field for SSRF's IDs, as shown in Fig.10. The same conclusion is obtained.

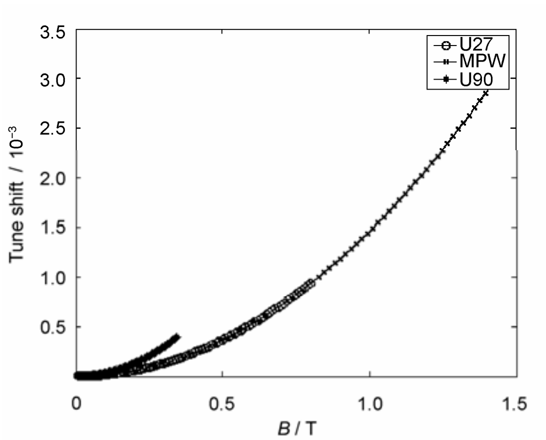


**Fig.10** Single ID's effect on tune shift for different fields.

## 4 Conclusions

We studied IDs' effects on SSRF storage ring both with theoretical analytical method and numerical stimulation Racetrack code. The result shows that their effects on dynamic aperture are small. This is because the beta functions in the middle of the straight sections, where IDs are located, are well optimized and the energy of beam is 3.5 GeV, high enough. Their total effect on beam emittance growth is –3%, and on beam energy spread is –0.3%.

## References

1 Robert A. Lattice and Emittance, CERN 98-04, 1998
2 SPEAR3 Concept Design Report, 8/30/99
3 Diamond Concept Design Report, July 2003
4 Martirosyan Y, Ivanyan M, Khachatryan M *et al*. Non-linear beam dynamics study in Candle light source, Proceedings of EPAC 2002, Paris, France
5 Walker R P. Insertion devices: undulators and wigglers, CERN 98-04, 1998
6 Wille K. Introduction to insertion devices, CERN 98-04, 1998
7 Iazzourene F. Racetrack user's guide, Version 4.01, July 1992
8 Wiedemann H. Particle Accelerator Physics, A USPAS PROGRAM, Vol. 2, 1998
9 Jin Yumin. Electron storage ring physics (in Chinese), University of Science and Technology of China Press, 2001
10 Helm R H, Lee M J, Morton P L. IEEE Trans Nucl Sci, 1973, NS-**20**: 3